Controllable synthesis of cuprite (Cu_2O) microcrystals and their shape-dependent photocatalytic performances

Peili Liu, Xu Zhang, Li Yao, Chengliang Han ✉

Department of Chemical and Material Engineering, Hefei University, Hefei, Anhui 230601, People's Republic of China
✉ *E-mail: clhan@issp.ac.cn*

Published in Micro & Nano Letters; Received on 18th July 2017; Revised on 17th March 2018; Accepted on 29th March 2018

Microcrystals of cuprite (Cu_2O) samples exhibiting octahedral and spherical morphologies were synthesised via a facile chemical method and were then characterised by X-ray powder diffraction and scanning electron microscopy. It was observed that the potassium sodium tartrate ($KNaC_4H_4O_6{\cdot}4H_2O$, PST) and gelatin addition had a prominent effect on the morphologies. The possible formation mechanism of Cu_2O microcrystals was discussed based on the effects of PST and gelatin. Furthermore, the photocatalytic activities of the prepared Cu_2O microcrystals were investigated by UV–vis spectrophotometry, demonstrating that their behavior was influenced by the different morphologies, and the Cu_2O microspheres possessed the highest activity.

1. Introduction: Cuprite (Cu_2O) is a direct bandgap semiconductor and its energy gap (E_g) is about 2.17 eV. Cu_2O can be applied in antiseptic, germicide, catalyst and colourant in daily life [1, 2]. In the past years, many methods have been used for obtaining Cu_2O with various morphologies [3–9]. Many reducing agents such as glucose [10–15], ascorbic acid [16–18], fructose [19], hydrazine hydrate [20–23], ureophil [3], glacial acetic acid [24], sodium borohydride [25] and polyol [26] will be introduced when copper salts (Cu^{2+}) are used as raw materials. Most of these reducing agents are usually expensive and toxic to some extent. Additionally, some organic compounds such as Polyvinylpyrrolidone (PVP) [27, 28] and Cetyltrimethylammonium bromide (CTAB) [29] have also been used as surfactants and templates to control the size and shape of Cu_2O. However, no reports can be found in the literature on the shape-controlled synthesis of Cu_2O microcrystals via PST reduction and gelatin templating control. Few works have been reported on photocatalytic degradation of micro-sized Cu_2O crystals.

In this study, a facile and environmental synthesising method has been presented. It has been found that PST can be used as an effective reduction to transform Cu^{2+} to Cu^{+} to form octahedral Cu_2O microcrystals in alkalic aqueous solution at low temperature. At the same time, spherical Cu_2O microcrystals will also be synthesised by using proper content of gelatin in alkaline solution of PST. The as-prepared Cu_2O microcrystals with different shapes have various UV–vis absorption properties and can be applied in effective removal of some dyes in wastewater.

2. Experiment section: All reagents are analytical grade and used without any further purification. In a typical chemical synthesis, 0.005 mol $CuSO_4{\cdot}5H_2O$ and 0.005 mol $KNaC_4H_4O_6{\cdot}4H_2O$ were added into 80 mL deionised water to from a light blue solution. Then, a dark blue solution was immediately acquired when 0.5 g NaOH was introduced to the above light blue solution. Finally, the above dark blue solution was heated for 3 h at 100°C in an oven and the octahedral Cu_2O microcrystals were obtained. Spherical Cu_2O microcrystals were prepared in the dark blue solution with 1.5 g gelatin. The phase, morphology, chemical composition and photoproperties of the as-prepared samples were characterised by the powder X-ray diffraction (XRD), scanning electron microscopy (SEM) equipped with an energy dispersive spectrometer (EDS) and UV–visible spectrophotometer (V-650, Jasco) at room temperature.

For the investigation of photocatalytic activity of Cu_2O microcrystals, 0.3 g Cu_2O was added to 200 mL rhodamine B (RhB) solution (10 mg/L) and vigorously stirred for 30 min in the dark to reach the adsorption–desorption equilibrium. Then, the above suspension was irradiated under a 300 W xenon lamp (PLS-SXE300) as a visible light source ($\lambda > 400$ nm). After irradiating for a certain time, 5 mL solution was taken out and be measured by a UV–vis absorption spectrum to acquire the concentration of RhB.

3. Results and discussion: Fig. 1 shows the XRD patterns of the prepared samples with different morphologies by a facile hydrothermal route. In the 2θ values of 29.4, 36.3, 42.3 and 61.3, the corresponding main characteristic d values of the XRD patterns for the samples of Cu_2O were 3.0377, 2.4778, 2.1436 and 2.0951 Å, respectively, which could be exactly indexed with those of JCPDS Card No. 05-0667 and thus showed an absence of other crystalline forms in the prepared samples. In comparison, the crystallinity of octahedral Cu_2O microcrystals is higher than that of spherical microcrystals, which can be deduced from the narrow half height wide from the (111) crystal plane.

The morphology and chemical composition of the synthesised Cu_2O microcrystals have been investigated by SEM and EDS. The corresponding results were indicated in Fig. 2. From Fig. 2*a*, it could be found that the Cu_2O microcrystals obtained from Cu(II)-PST precursor solutions exhibited an octahedral shape and the average size of each crystal was about 1–3 µm. The eight crystal planes for each octahedron have been researched and considered to be a (111) crystal face family ({111}) [22]. Figs. 2*c* and *d* illustrated sphere-like Cu_2O microcrystals with an average diameter of 1–2 µm which were prepared from Cu (II)-PST solution with 1.5 g gelatin. Every microsphere was consisted of lots of Cu_2O nanoparticles and has a rough surface and porous structure. Chemical compositions of octahedral and spherical microcrystals are Cu and O which were shown in different modes in Figs. 2*b* and *d*, respectively.

The UV–vis spectrums of two-shaped Cu_2O microcrystals were carried out and shown in Fig. 3*a*. Comparing the results, it can be found that the maximum absorption wavelengths for octahedral and spherical Cu_2O microcrystals are at 550 and 750 nm, respectively. Their corresponding bandgap energies (E_g) could be estimated on the following equation [24] and the results were figured out in Fig. 3*b*

$$\alpha E_{\text{photon}} = K(E_{\text{photon}} - E_g)^{1/2}$$

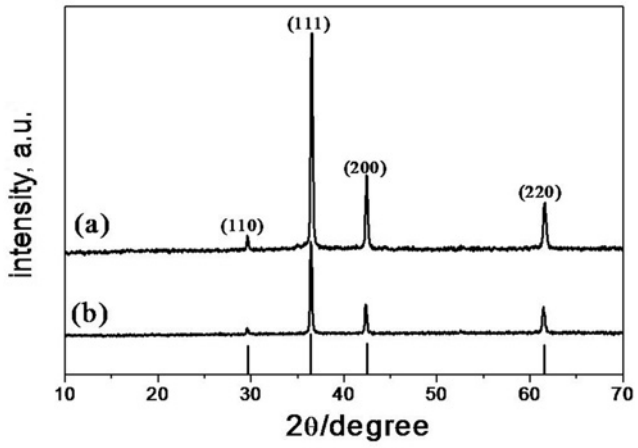

Fig. 1 *XRD patterns of the as-prepared samples*
a Octahedral microcrystals
b Spherical microcrystals

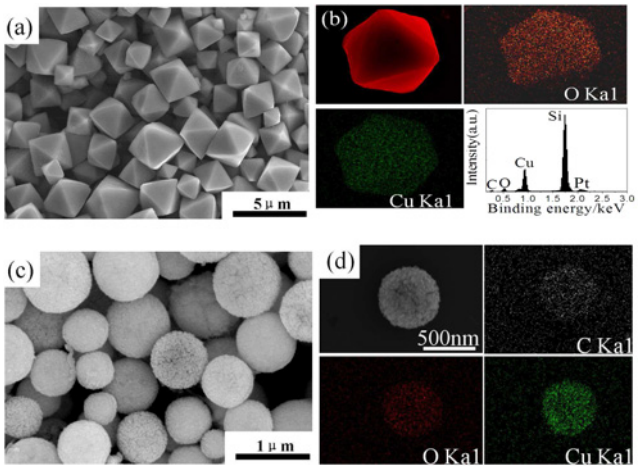

Fig. 2 *SEM images and EDS analysis of the samples*
a, *b* Octahedral microcrystals
c, *d* Spherical microcrystals

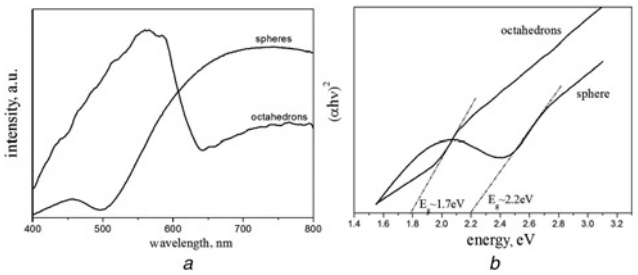

Fig. 3 *UV-vis. Spectrums of Cu_2O microcrystals with different shapes*
a UV-vis. absorption spectrums
b Their corresponding curves of curves of $(\alpha hv)^2 \sim hv$

where K and α are a constant and the absorption coefficient, E_{photon} and E_g are the discrete photoenergy and the bandgap energy. The energy intercept of a plot of $(\alpha E_{photon})^2$ versus E_{photon} will produce E_g for a direct bandgap semiconductor. It can be estimated that the E_g of the as-prepared octahedral and spherical Cu_2O microcrystals are 1.7 and 1.5 eV which are all lower than that of the bulk Cu_2O(~2.2 eV) [22]. The shaped and sized effects of Cu_2O powders were also observed.

In next experiments, the role of PST in the formation of Cu_2O microcrystals was researched. First of all, PST would reduce Cu^{2+} to Cu^{+}which formed Cu_2O at 100°C. Secondly, some irregular Cu_2O particles would be obtained when the content of PST was too much or too little in the reaction systems (seen from Fig. 4). That is to say, proper content of PST is beneficial to the formation of Cu_2O octahedrons. The proper concentration of PST will control the supply of Cu^{+} ions, which affect the formation of Cu_2O in the reaction. Therefore, it can be concluded that the PST plays double roles in controlling the phase and morphology. Additionally, some irregular Cu_2O crystals will be obtained due to lower pH values (pH = 4–6) and higher pH values (pH = 9–14) in the reaction systems when the insufficient or excess PST was used, which is valued to be further studied in our next work.

It has been known that the gelatin can be used as an effective template to control the shape of Fe_3O_4 nanomaterials [30]. In the preparation of Cu_2O, it was also found that the used gelatin could effectively make Cu_2O octahedrons turn into Cu_2O microspheres in the reaction progress. A content of gelatin influencing on shapes of Cu_2O microcrystals was figured out in Fig. 5. It further proves that too much or little content of gelatin is bad for generating pure spherical Cu_2O microcrystals.

Based on the above experimental results, the possible formation mechanism of octahedral and spherical Cu_2O microcrystals was illustrated in Fig. 6. For octahedral Cu_2O microcrystals, Firstly, small Cu_2O octahedrons will be slowly generated due to the lower release of Cu^{+} ions in the solution. The supersaturation concentration of Cu^{+} ions will be controlled by $Cu_2C_4H_4O_6$ species produced from Cu^{+} and $C_4H_4O_6^{2-}$ ions. Accordingly, the initially formed nano-sized Cu_2O octahedrons can further grow into larger ones via the Ostwald ripening process. However, the above formation process will be changed due to introduction of gelatin to the reaction system. The added gelatin can be regarded as effective templates for assembling the formed Cu_2O nanoparticles into microspheres in order to reduce their surface energy. These Cu_2O microspheres produced by inter-particle aggregations exhibit a polycrystalline microstructure.

To demonstrate the potential application of the as-prepared Cu_2O microcrystals, the octahedral and spherical Cu_2O microcrystals were comparatively used as photocatalysts for degradation of

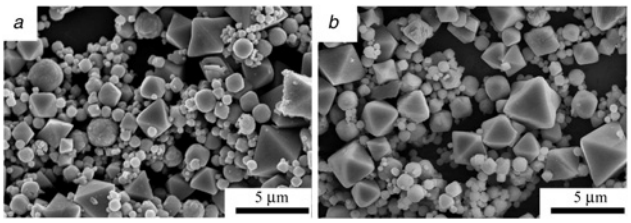

Fig. 4 *Contents of reductive agents (PST) influencing on shapes of Cu_2O microcrystals*
a 0.001 mol
b 0.01 mol

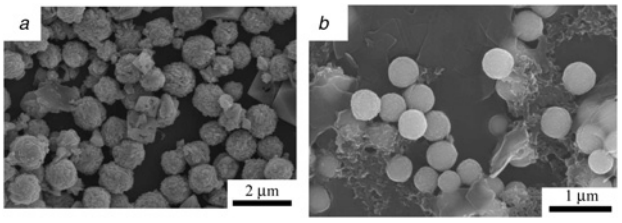

Fig. 5 *Contents of gelatin influencing on shapes of Cu_2O microcrystals*
a 0.5 g
b 2 g

doi: 10.1049/mnl.2017.0495

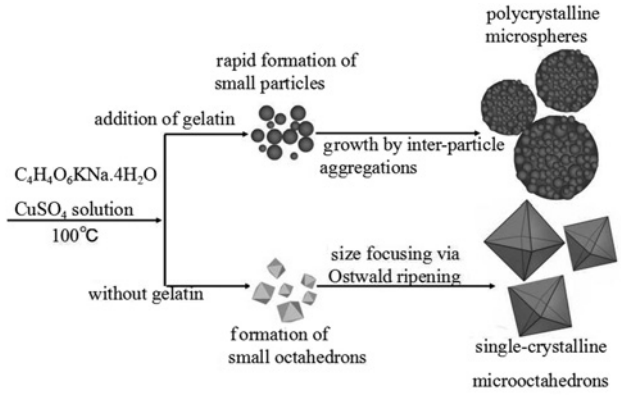

Fig. 6 *Schematic illustration of the reaction pathways that lead to the formation of octahedral and spherical Cu_2O microcrystals*

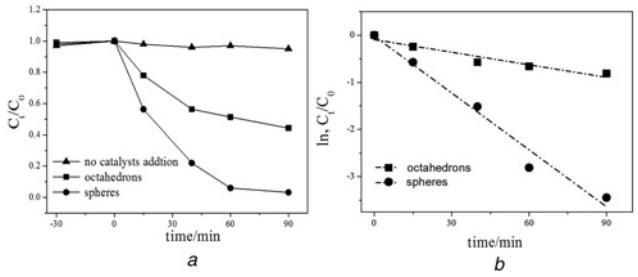

Fig. 7 *Photodegradation efficiencies of RhB as a function of irradiation time over different samples*
a Plot of C_t/C_0 versus irradiation time
b Plot of ln (C_t/C_0) versus irradiation time

RhB in water, respectively. As illustrated in Fig. 7*a*, for two-shaped catalysts, the relative concentration of the RhB (C_t/C_0) will gradually decrease with the irradiation time (t). The fitted lines ($\ln(C_t/C_0) \sim t$) mean that the photocatalytic process can be expressed by a pseudo-first-order kinetic model (seen from Fig. 7*b*) which has been reported in previous literatures [30–33]. In comparison, Cu_2O microspheres have relative higher photocatalytic performance due to their special micro/nanostructure which had the lower bandgap.

The previous references have reported that the octahedral Cu_2O crystals show a higher activity in the photodegradation of organic pollutes [33, 34]. However, our results reveal that the different photodegradation activities of octahedral and spherical Cu_2O microcrystals arise from their intrinsic differences in the crystallographic structures, in which the spherical Cu_2O crystals possess more interfaces. Therefore, the photocatalytic superiority of the spherical Cu_2O crystals can be attributed to the introduction of many active interfaces in the Cu_2O microspheres, which can accelerate the formation of highly oxidative .OH radicals, leading to the enhancement of the decomposition of RhB dyes.

4. Conclusion: In summary, a novel approach for preparing micro-sized Cu_2O was presented. Octahedral Cu_2O microcrystals could be prepared in Cu(II)–$C_4H_4O_6KNa$–NaOH system. However, spherical Cu_2O microcrystals could be obtained from the above reaction system with proper gelatin addition. The $C_4H_4O_6KNa{\cdot}4H_2O$ and the added gelatin played reductive, shape-controlling and template roles, respectively. Cu_2O microspheres have relative higher photocatalytic performance than that of octahedral Cu_2O microcrystals. This easy method will propose a new way to synthesise micro/nanostructured materials.

5. Acknowledgments: This work was supported by the Natural Science Foundation of Hefei University (grant no. 16ZR10ZDA) and the Key Projects of Anhui Province University Outstanding Youth Talent Support Program (grant no. gxyqZD2016271) and the National College Students Innovation Project (grant no. 201611059019).

6 References

[1] Park K.-S., Seo S.-D., Jin Y.-H., *ET AL.*: 'Synthesis of cuprous oxide nanocomposite electrodes by room-temperature chemical partial reduction', *Dalton Trans.*, 2011, **40**, pp. 9498–9503
[2] Kwon Y., Soon A., Han H., *ET AL.*: 'Shape effects of cuprous oxide particles on stability in water and photocatalytic water splitting', *J. Mater. Chem. A*, 2015, **3**, pp. 156–159
[3] Ma Z.-C., Wang L.-M., Chu D.-Q., *ET AL.*: 'Template-free synthesis of complicated doublewall Cu_2O hollow spheres with enhanced visible photocatalytic activities', *RSC Adv.*, 2015, **5**, pp. 8223–8227
[4] Soroka I.L., Tarakina N.V., Korzhavyi P.A., *ET AL.*: 'Effect of synthesis temperature on the morphology and stability of copper(I) hydride nanoparticles', *CrystEngComm*, 2013, **15**, pp. 8450–8453
[5] Wang Q., Kuang Q., Wang K., *ET AL.*: 'A surfactant free synthesis and formation mechanism of hollow Cu_2O nanocubes using Cl^- ions as the morphology regulator', *RSC Adv.*, 2015, **5**, pp. 61421–61425
[6] Bai L., Dang Z.: 'Facile synthesis of litchi shaped cuprous oxide and its application in the aerobic oxidative synthesis of imines', *RSC Adv.*, 2015, **5**, pp. 10341–10343
[7] Nunes D., Pimentel A., Barquinha P., *ET AL.*: 'Cu_2O polyhedral nanowires produced by microwave irradiation', *J. Mater. Chem. C*, 2014, **2**, pp. 6097–6100
[8] Leng M., Yua C., Wang C.: 'Polyhedral Cu_2O particles: shape evolution and catalytic activity on cross-coupling reaction of iodobenzene and phenol', *CrystEngComm*, 2012, **14**, pp. 8454–8461
[9] Wang X., Liu C., Zheng B., *ET AL.*: 'Controlled synthesis of concave Cu_2O microcrystals enclosed by {hhl} high-index facets and enhanced catalytic activity', *J. Mater. Chem. A*, 2013, **1**, pp. 282–285
[10] Li H., Ni Y., Cai Y., *ET AL.*: 'Ultrasound-assisted preparation, characterization and properties of porous Cu_2O microcubes', *J. Mater. Chem.*, 2009, **19**, pp. 594–597
[11] Liang Y., Shang L., Bian T., *ET AL.*: 'Shape-controlled synthesis of polyhedral 50-facet Cu_2O microcrystals with high-index facets', *CrystEngComm*, 2012, **14**, pp. 4431–4436
[12] Li S.-K., Guo X., Wang Y., *ET AL.*: 'Rapid synthesis of flower-like Cu_2O architectures in ionic liquids by the assistance of microwave irradiation with high photochemical activity', *Dalton Trans.*, 2011, **40**, pp. 6745–6750
[13] Li R., Yan X., Yu L., *ET AL.*: 'The morphology dependence of cuprous oxide and its photocatalytic properties', *CrystEngComm*, 2013, **15**, pp. 10049–10052
[14] Prabhakaran G., Murugan R.: 'Synthesis of Cu_2O microcrystals with morphological evolution from octahedral to microrod through a simple surfactant-free chemical route', *CrystEngComm*, 2012, **14**, pp. 8338–8341
[15] Chen K., Xue D.: 'pH-assisted crystallization of Cu_2O: chemical reactions control the evolution from nanowires to polyhedral', *CrystEngComm*, 2012, **14**, pp. 8068–8075
[16] Wan X., Wang J., Zhu L., *ET AL.*: 'Gas sensing properties of Cu_2O and its particle size and morphology-dependent gas-detection sensitivity', *J. Mater. Chem. A*, 2014, **2**, pp. 13641–13647
[17] Fan X., Hua N., Xu J., *ET AL.*: 'Controllable synthesis of two different morphologies of Cu_2O particles with the assistance of carbon dots', *RSC Adv.*, 2014, **4**, pp. 16524–16527
[18] Theja G.S., Lowrence R.C., Ravi V., *ET AL.*: 'Synthesis of Cu_2O micro/nanocrystals with tunable morphologies using coordinating ligands as structure controlling agents and antimicrobial studies', *CrystEngComm*, 2014, **16**, pp. 9866–9872
[19] Zheng H., Li Q., Yang C., *ET AL.*: 'Controllable green synthesis of Cu_2O nanocrystals with shape evolution from octahedra to truncated octahedral', *RSC Adv.*, 2015, **5**, pp. 59349–59353
[20] Wang W., Zhang P., Peng L., *ET AL.*: 'Template-free room temperature solution phase synthesis of Cu_2O hollow spheres', *CrystEngComm*, 2010, **12**, pp. 700–701
[21] Zhang N., Du Y., Zhang Y., *ET AL.*: 'A simple method for controlling the type of cuprous oxide semiconductors using different surfactants', *J. Mater. Chem.*, 2011, **21**, pp. 5408–5413
[22] Tsai Y.-H., Chanda K., Chu Y.-T., *ET AL.*: 'Direct formation of small Cu_2O nanocubes, octahedra, and octapods for efficient synthesis of triazoles', *Nanoscale*, 2014, **6**, pp. 8704–8709

[23] Chen K., Xue D.: 'Chemoaffinity-mediated crystallization of Cu_2O: a reaction effect on crystal growth and anode property', *CrystEngComm*, 2013, **15**, pp. 1739–1746
[24] Jiang Y., Kong D., Zhao J., *ET AL.*: '$Cu(OAc)_2{\cdot}H_2O/NH_2NH_2{\cdot}H_2O$: an efficient catalyst system that in situ generates Cu_2O nanoparticles and HOAc for Huisgen click reactions', *RSC Adv.*, 2014, **4**, pp. 1010–1014
[25] Meng X., Tian G., Chen Y., *ET AL.*: 'Room temperature solution synthesis of hierarchical bow-like Cu_2O with high visible light driven photocatalytic activity', *RSC Adv.*, 2012, **2**, pp. 2875–2881
[26] Kim M.H., Lim B., Lee E.P., *ET AL.*: 'Polyol synthesis of Cu_2O nanoparticles: use of chloride to promote the formation of a cubic morphology', *J. Mater. Chem.*, 2008, **18**, pp. 4069–4073
[27] Zhang D.-F., Zhang H., Guo L., *ET AL.*: 'Delicate control of crystallographic facet-oriented Cu_2O nanocrystals and the correlated adsorption ability', *J. Mater. Chem.*, 2009, **19**, pp. 5220–5225
[28] Yang L., Sui Y., Zhao W., *ET AL.*: 'One-pot shorter time synthesis of Cu_2O particles and nanoframes with novel shapes', *CrystEngComm*, 2011, **13**, pp. 6265–6270
[29] Sui Y., Zeng Y., Fu L., *ET AL.*: 'Low-temperature synthesis of porous hollow structured Cu_2O for photocatalytic activity and gas sensor application', *RSC Adv.*, 2013, **3**, pp. 18651–18660
[30] Han C., Cai W., Tang W., *ET AL.*: 'Protein assisted hydrothermal synthesis of ultrafine magnetite nanoparticle built-porous oriented fibers and their structurally enhanced adsorption to toxic chemicals in solution', *J. Mater. Chem.*, 2011, **21**, pp. 11188–11196
[31] Ghiasi M., Malekzadeh A.: 'Solar photocatalytic degradation of methyl orange over $La_{0.7}Sr_{0.3}MnO_3$ nano-perovskite', *Sep. Purif. Technol.*, 2014, **134**, pp. 12–19
[32] Zhang Y., Gu J., Murugananthan M., *ET AL.*: 'Development of novel α-$Fe_2O_3/NiTiO_3$ heterojunction nanofibers material with enhanced visible-light photocatalytic performance', *J. Alloys Compd.*, 2015, **630**, pp. 110–116
[33] Zhang Y., Deng B., Zhang T., *ET AL.*: 'Shape effects of Cu_2O polyhedral microcrystals on photocatalytic activity', *J. Phys. Chem. C*, 2010, **114**, pp. 5073–5079
[34] Sun S., Song X., Sun Y., *ET AL.*: 'The crystal-facet-dependent effect of polyhedral Cu_2O microcrystals on photocatalytic activity', *Catal. Sci. Technol.*, 2012, **2**, pp. 925–930

doi: 10.1049/mnl.2017.0495